

Towards Quantum Communication with Electron Spins

D.S. SARAGA¹, G. BURKARD², J. C. EGUES³, H.-A. ENGEL¹,
P. RECHER¹, D. LOSS¹

¹*Department of Physics and Astronomy, University of Basel
Klingelbergstrasse 82, 4056 Basel, Switzerland*

²*IBM T. J. Watson Research Center, P. O. Box 218, Yorktown Heights, NY 10598*

³*Department of Physics and Informatics, University of São Paulo at São Carlos,
13560-970 São Carlos/SP, Brazil*

Received 11.09.2003

Abstract

We review our recent work towards quantum communication in a solid-state environment with qubits carried by electron spins. We propose three schemes to produce spin-entangled electrons, where the required separation of the partner electrons is achieved via Coulomb interaction. The non-product spin-states originate either from the Cooper pairs found in a superconductor, or in the ground state of a quantum dot with an even number of electrons. In a second stage, we show how spin-entanglement carried by a singlet can be detected in a beam-splitter geometry by an increased (bunching) or decreased (antibunching) noise signal. We also discuss how a local spin-orbit interaction can be used to provide a continuous modulation of the noise as a signature of entanglement. Finally, we review how one can use a quantum dot as a spin-filter, a spin-memory read-out, a probe for single-spin decoherence and, ultimately, a single-spin measurement apparatus.

1. Introduction

The goal of the growing field of spintronics [1, 2] is to harness the spin degree-of-freedom of the electron in a solid-state environment. By going beyond the manipulation of the electron charge found in standard electronics, one pursues the development of new devices that use specifically the electron spin: for instance, magnetic read-out heads for computer hard drives, single-spin memories, or spin transistors [3, 4]. One ingredient is the injection and detection of spin-polarized currents, which has now been studied experimentally with various approaches [5, 6, 7]. A more ambitious step is to consider quantum computation [8], for which it has been proposed to use the electron spin as a qubit [9]. This naturally requires coherent manipulation of the quantum spin-state, which is limited by decoherence. The issue of electron spin decoherence in semiconductors has found positive support from a number of experiments, which have now demonstrated long decoherence times (exceeding 100 ns) for electron spins in bulk n-doped GaAs, as well as coherent transport of spins over distances up to 100 μm [11]. In this work, we address the most fundamental issues concerning the use of the electron spin in quantum communication [10], the basic resource being Einstein-Podolsky-Rosen (EPR) pairs [12]. Here the motivation stems from for the desire to use the same physical qubit as the one used for quantum computation [9], in order to have “on-chip” quantum communication without transfers to photonic states. Secondly, these efforts open the path towards experimental tests of quantum non-locality with massive particles in the solid state (via violation of Bell’s inequality [13]).

The first challenge is to create pairs of entangled electrons such as EPR pairs—that is, electrons whose quantum state cannot be written as a product state, and where the two electrons are separately addressable because of their spatial separation [14]. We describe in Section 2 how this can be achieved by extracting a Cooper pair from a superconductor [15, 16] or the singlet ground state of a quantum dot with an even

number of electrons [17]. The separation of the two electrons into distinct channels can be achieved with the help of interactions found in nanostructures, such as the Coulomb blockade occurring in quantum dots [15, 17], or the Coulomb repulsion in one-dimensional quantum wires [16]. In Section 3 we address the issue of the measurement of entanglement, and describe a simple beam-splitter setup [18, 19, 20] where a noise measurement can distinguish spin-singlet states from spin-triplets by probing the symmetry of the orbital part of the electron-pair wavefunction. We describe in Section 4 how spin-filtering can be achieved with the help of a quantum dot [21]. Such a device can also lead to the read-out of a spin-memory carried by an electron in a quantum dot [21], and to the measurement of the decoherence rate of single spin in a quantum dot via electron spin resonance and energy filtering [22]. We also refer the reader to our previous reviews [23, 24], which the present article follows closely.

2. Producing mobile spin-entangled electrons

Quantum communication schemes and experimental tests of quantum non-locality require entangled particles on demand, which is the motivation for a number of theoretical proposals [15, 16, 17, 25, 26, 27, 28, 29, 30, 31] for of an electron “entangler” —a device creating mobile entangled electrons which are spatially separated. Interestingly, entanglement is rather the rule than the exception in nature, as it is a direct consequence from Fermi statistics. For instance, the ground state of a Helium atom is the spin singlet $|\uparrow\downarrow\rangle - |\downarrow\uparrow\rangle$. The corresponding “artificial atom” [32], a quantum dot with two electrons, has also a singlet ground state.

However, such “local” entangled singlets are not readily useful for quantum computation and communication, which require control over each individual electron as well as non-local correlations. In a first setup —which has now been implemented experimentally [33]— one has considered two coupled quantum dots with a single electron in each dot, where the spin-entangled electrons are already spatially separated by strong on-site Coulomb repulsion (like in a Hydrogen molecule) [9]. Mobile entangled electrons could then be obtained by simultaneously lowering the tunnel barriers coupling each dot to separate leads. Another source of spin entanglement is provided by superconductors containing Cooper pairs in the spin-singlet state. It was first shown in Ref. [25] how a non-local entangled state is created in two uncoupled quantum dots when coupled to the same superconductor. In a non-equilibrium situation, the Cooper pairs can be extracted to normal leads by Andreev tunnelling, thus creating a flow of entangled pairs [15, 16, 26, 27, 28, 29]

A crucial requirement for an entangler is to create *spatially separated* entangled electrons; hence one must avoid whole entangled pairs entering the same lead. As it will be shown below, an efficient mechanism for the suppression of undesired channels is provided by energy conservation and interactions —for instance, Coulomb repulsion in quantum dots [15, 17] or in Luttinger liquids [16, 26]. Other recent spin-entangler proposals used interferences in a quantum dot [30] or beam-splitters for spin-polarized currents [31]. Recently, a simple tunneling barrier for edge states in the quantum Hall effect has been proposed to generate particle-hole entanglement [34]. In the following, we discuss our proposals towards the realization of an entangler that produces mobile non-local spin singlets [35].

2.1. Superconductor-based electron entanglers

Here we envision a *non-equilibrium* situation in which the electrons of a Cooper pair tunnel coherently by means of an Andreev tunnelling event from a superconductor (SC) to two separate normal leads, one electron per lead. Due to an applied bias voltage, the electron pairs can move into the leads thus giving rise to mobile spin entanglement. Note that an (unentangled) single-particle current is strongly suppressed by energy conservation as long as both the temperature and the bias are much smaller than the superconducting gap. In the following we review two proposals where we exploit the repulsive Coulomb charging energy between the two spin-entangled electrons in order to separate them so that the residual current in the leads is carried by non-local singlets. We show that such entanglers meet all requirements for subsequent detection of spin-entangled electrons via noise measurements of the charge current (see Sec. 3) or via single-spin measurements (see Sec. 4), which could be used to perform experimental tests of Bell’s inequality.

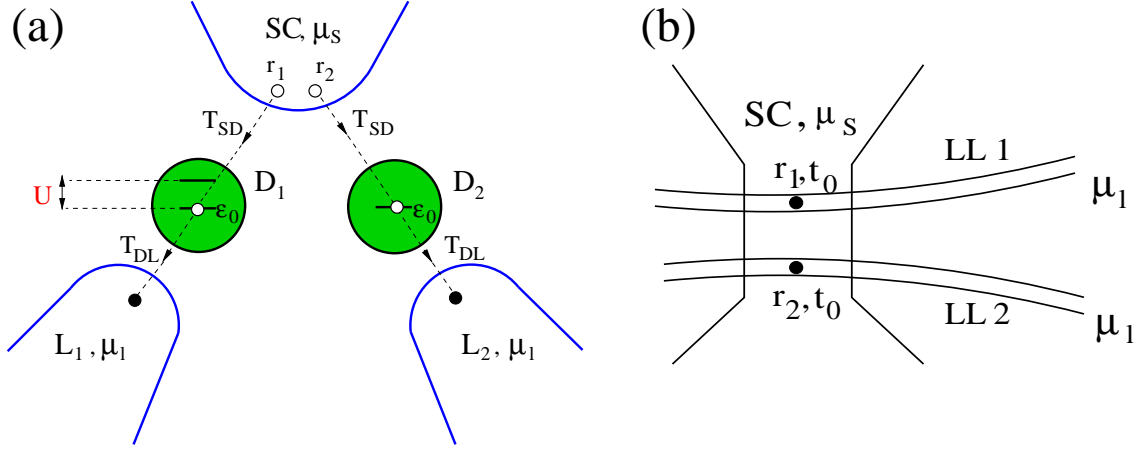


Figure 1. (a) Setup of the superconductor-double dot entangler. Two spin-entangled electrons forming a Cooper pair in the superconductor SC tunnel (with amplitude T_{SD} and from the points \mathbf{r}_1 and \mathbf{r}_2) to two quantum dots D_1 and D_2 . The electrons then tunnel to normal Fermi liquid leads L_1 and L_2 , with tunnelling amplitude T_{DL} . The superconductor and leads are kept at chemical potentials μ_S and μ_l . (b) An s-wave superconductor SC (at chemical potential μ_S) is in contact with two quantum wires LL1 and LL2, which are described as infinitely long Luttinger liquids (LL) (at chemical potential μ_l). The electrons of a Cooper pair can tunnel by means of an Andreev process from two points \mathbf{r}_1 and \mathbf{r}_2 on the SC to the center (bulk) of the two quantum wires 1 and 2, respectively, with tunnelling amplitude t_0 . Adapted from [15, 16].

2.1.1. Andreev entangler with quantum dots

The proposed entangler setup is described in Fig. 1(a). It consists of a SC with chemical potential μ_S which is weakly coupled to two quantum dots (QDs) in the Coulomb blockade regime [32]. These QDs are in turn weakly coupled to outgoing Fermi liquid leads, held at the same chemical potential μ_l . A bias voltage $\Delta\mu = \mu_S - \mu_l$ is applied between the SC and the leads. The tunnelling amplitudes between the SC and the dots, and between the dots and the leads, are denoted by T_{SD} and T_{DL} , respectively; see Fig. 1(a). The two intermediate QDs in the Coulomb blockade regime have chemical potentials ϵ_1 and ϵ_2 . These can be tuned via external gate voltages, such that the tunnelling of two electrons via different dots into different leads is resonant for $\epsilon_1 + \epsilon_2 = 2\mu_S$ [36]. As it turns out [15], this two-particle resonance is suppressed for the tunnelling of two electrons via the same dot into the same lead by the on-site repulsion U of the dots and/or the superconducting gap Δ . Next, we specify the parameter regime of interest here in which the initial spin-entanglement of a Cooper pair in the SC is successfully transported to the leads.

Besides the fact that single-electron tunnelling and tunnelling of two electrons via the same dot should be excluded, we also have to suppress transport of electrons which are already on the QDs. This could lead to effective spin-flips on the QDs, which would destroy the spin entanglement of the two electrons tunnelling into the Fermi leads. A further source of unwanted spin-flips on the QDs is provided by its coupling to the Fermi liquid leads via particle-hole excitations in the leads. The QDs can be treated each as one localized spin-degenerate level as long as the mean level spacing $\delta\epsilon$ of the dots exceeds both the bias voltage $\Delta\mu$ and the temperature $k_B T$. In addition, we require that each QD contains an even number of electrons with a spin-singlet ground state. A more detailed analysis of such a parameter regime is given in [15] and is stated here

$$\Delta, U, \delta\epsilon > \Delta\mu > \gamma_l, k_B T \quad \text{and} \quad \gamma_l > \gamma_S. \quad (1)$$

In (1) the rates for tunnelling of an electron from the SC to the QDs and from the QDs to the Fermi leads are given by $\gamma_S = 2\pi\nu_S|T_{SD}|^2$ and $\gamma_l = 2\pi\nu_l|T_{DL}|^2$, respectively, with ν_S and ν_l being the corresponding electron density of states per spin at the Fermi level. We consider asymmetric barriers $\gamma_l > \gamma_S$ in order to exclude correlations between subsequent Cooper pairs on the QDs. We work at the particular interesting resonance $\epsilon_1, \epsilon_2 \simeq \mu_S$, where the injection of the electrons into different leads takes place at the same orbital

energy. This is a crucial requirement for the subsequent detection of entanglement via noise [18, 19, 20]; see Sec. 3. In this regime, we have calculated and compared the stationary charge current of two spin-entangled electrons for two competing transport channels in a T-matrix approach.

The ratio of the desired current for two electrons tunnelling into *different* leads (I_1) to the unwanted current for two electrons into the *same* lead (I_2) is [15]

$$\frac{I_1}{I_2} = \frac{4\mathcal{E}^2}{\gamma^2} \left[\frac{\sin(k_F \delta r)}{k_F \delta r} \right]^2 e^{-2\delta r/\pi\xi}, \quad \frac{1}{\mathcal{E}} = \frac{1}{\pi\Delta} + \frac{1}{U}, \quad (2)$$

where $\gamma = \gamma_1 + \gamma_2$. The current I_1 becomes exponentially suppressed with increasing distance $\delta r = |\mathbf{r}_1 - \mathbf{r}_2|$ between the tunnelling points on the SC, on a scale given by the superconducting coherence length ξ which is the size of a Cooper pair. This does not pose a severe restriction for conventional s-wave materials with ξ typically being on the order of μm . In the relevant case $\delta r < \xi$ we find a slower, power-law suppression $\propto 1/(k_F \delta r)^2$, where k_F is the Fermi wave vector in the SC. On the other hand, we see that the effect of the QDs consists in the suppression factor $(\gamma/\mathcal{E})^2$ for tunnelling into the same lead [37]. Thus, in addition to Eq. (1) we have to impose the condition $k_F \delta r < \mathcal{E}/\gamma$, which can be satisfied for small dots with $\mathcal{E}/\gamma \sim 100$ and $k_F^{-1} \sim 1 \text{ \AA}$. As an experimental probe to test if the two spin-entangled electrons indeed separate and tunnel to different leads we suggest to join the two leads 1 and 2 to form an Aharonov-Bohm loop. In such a setup the different tunnelling paths of an Andreev process from the SC via the dots to the leads can interfere. As a result, the measured current as a function of the applied magnetic flux ϕ threading the loop contains a phase coherent part I_{AB} which consists of oscillations with periods h/e and $h/2e$ [15]

$$I_{AB} \sim \sqrt{8I_1 I_2} \cos(\phi/\phi_0) + I_2 \cos(2\phi/\phi_0), \quad (3)$$

with $\phi_0 = h/e$ being the single-electron flux quantum. The ratio of the two contributions scales like $\sqrt{I_1/I_2}$ which suggest that by decreasing I_2 (e.g. by increasing U) the $h/2e$ oscillations should vanish faster than the h/e ones.

We note that the efficiency as well as the absolute rate for the desired injection of two electrons into different leads can even be enhanced by using lower dimensional SCs [16]. In two dimensions (2D) we find that $I_1 \propto 1/k_F \delta r$ for large $k_F \delta r$, and in one dimension (1D) there is no suppression of the current and only an oscillatory behavior in $k_F \delta r$ is found. A 2D-SC can be realized by using a SC on top of a two-dimensional electron gas (2DEG) [38], where superconducting correlations are induced via the proximity effect in the 2DEG. In 1D, superconductivity was found in ropes of single-walled carbon nanotubes [39].

Finally, we note that the coherent injection of Cooper pairs by an Andreev process allows the detection of individual spin-entangled electron pairs in the leads. The delay time τ_{delay} between the two electrons of a pair is given by $1/\Delta$, whereas the separation in time of subsequent pairs is given approximately by $\tau_{\text{pairs}} \sim 2e/I_1 \sim \gamma_l/\gamma_S^2$ (up to geometrical factors) [15]. For $\gamma_S \sim \gamma_l/10 \sim 1\mu\text{eV}$ and $\Delta \sim 1\text{meV}$ we obtain that the delay time $\tau_{\text{delay}} \sim 1/\Delta \sim 1\text{ps}$ is much smaller than the delivery time τ_{pairs} per entangled pair $2e/I_1 \sim 40\text{ns}$. Such a time separation is indeed necessary in order to detect individual pairs of spin-entangled electrons.

2.1.2. Andreev entangler with Luttinger-liquid leads

In Fig. 1(b) we propose a setup with an s-wave SC weakly coupled to the center (bulk) of two separate one-dimensional leads (quantum wires) 1,2 which exhibit Luttinger liquid (LL) behavior, such as carbon nanotubes [40]. The leads are assumed to be infinitely extended and are described by conventional LL-theory [41]. Interacting electrons in one dimension lack the existence of quasi particles as in a Fermi liquid and instead the low energy excitations are collective charge and spin modes. In the absence of backscattering interaction the velocities of the charge and spin excitations are given by $u_\rho = v_F/K_\rho$ for the charge and $u_\sigma = v_F$ for the spin, where v_F is the Fermi velocity and $K_\rho < 1$ for repulsive interaction between electrons ($K_\rho = 1$ corresponds to a 1D-Fermi gas). As a consequence of this non-Fermi liquid behavior, tunnelling into a LL is strongly suppressed at low energies. Therefore one should expect additional interaction effects in a two-particle tunnelling event (Andreev process) of a Cooper pair from the SC to the leads. We find

that strong LL-correlations result in an additional suppression for tunnelling of two coherent electrons into the *same* LL compared to single electron tunnelling into a LL if the applied bias voltage μ between the SC and the two leads is much smaller than the energy gap Δ of the SC.

To quantify the effectiveness of such an entangler, we calculate the current for the two competing processes of tunnelling into different leads (I_1) and into the same lead (I_2) in lowest order via a tunnelling Hamiltonian approach. Again we account for a finite distance separation δr between the two exit points on the SC when the two electrons of a Cooper pair tunnel to different leads. For the current I_1 of the desired pair-split process we obtain, in leading order in μ/Δ and at zero temperature [16]

$$I_1 = \frac{I_1^0}{\Gamma(2\gamma_\rho + 2)} \frac{v_F}{u_\rho} \left[\frac{2\Lambda\mu}{u_\rho} \right]^{2\gamma_\rho}, \quad I_1^0 = \pi e \gamma^2 \mu F_d[\delta r], \quad (4)$$

where $\Gamma(x)$ is the Gamma function and Λ is a short distance cut-off on the order of the lattice spacing in the LL and $\gamma = 4\pi\nu_S\nu_l|t_0|^2$ is the dimensionless tunnel conductance per spin with t_0 being the bare tunnelling amplitude for electrons to tunnel from the SC to the LL-leads; see Fig. 1(b). The electron density of states per spin at the Fermi level for the SC and the LL-leads are denoted by ν_S and ν_l , respectively. The current I_1 has its characteristic non-linear form $I_1 \propto \mu^{2\gamma_\rho+1}$ with $\gamma_\rho = (K_\rho + K_\rho^{-1})/4 - 1/2 > 0$ being the exponent for tunnelling into the bulk of a *single* LL. The factor $F_d[\delta r]$ in (4) depends on the geometry of the device and is given here again by $F_d[\delta r] = [\sin(k_F\delta r)/k_F\delta r]^2 \exp(-2\delta r/\pi\xi)$ for the case of a 3D-SC. In complete analogy to subsection 2.1.1 the power law suppression in $k_F\delta r$ gets weaker in lower dimensions.

This result should be compared with the unwanted transport channel where two electrons of a Cooper pair tunnel into the same lead 1 or 2 but with $\delta r = 0$. We find that such processes are indeed suppressed by strong LL-correlations if $\mu < \Delta$. The result for the current ratio I_2/I_1 in leading order in μ/Δ and for zero temperature is [16]

$$\frac{I_2}{I_1} = F_d^{-1}[\delta r] \sum_{b=\pm 1} A_b \left(\frac{2\mu}{\Delta} \right)^{2\gamma_{\rho b}}, \quad \gamma_{\rho+} = \gamma_\rho, \quad \gamma_{\rho-} = \gamma_\rho + (1 - K_\rho)/2, \quad (5)$$

where A_b is an interaction dependent constant [42]. The result (5) shows that the current I_2 for injection of two electrons into the same lead is suppressed compared to I_1 by a factor of $(2\mu/\Delta)^{2\gamma_{\rho+}}$, if both electrons are injected into the same branch (left or right movers), or by $(2\mu/\Delta)^{2\gamma_{\rho-}}$ if the two electrons travel in different directions [43]. The suppression of the current I_2 by $1/\Delta$ reflects the two-particle correlation effect in the LL, when the electrons tunnel into the same lead. The larger Δ , the shorter the delay time is between the arrivals of the two partner electrons of a Cooper pair, and, in turn, the more the second electron tunnelling into the same lead will feel the existence of the first one which is already present in the LL. This behavior is similar to the Coulomb blockade effect in QDs discussed in the previous subsection. Concrete realizations of LL-behavior are found in metallic carbon nanotubes with similar exponents as derived here [40]. In metallic single-walled carbon nanotubes $K_\rho \sim 0.2$ [40], which corresponds to $2\gamma_\rho \sim 1.6$. This suggests the rough estimate $(2\mu/\Delta) < 1/k_F\delta r$ for the entangler to be efficient. As a consequence, voltages in the range $k_B T < \mu < 100\mu\text{eV}$ are required for $\delta r \sim \text{nm}$ and $\Delta \sim 1\text{meV}$. In addition, nanotubes were reported to be very good spin conductors [44] with estimated spin-flip scattering lengths of the order of μm [26].

We remark that in order to use the beam-splitter setup to detect spin-entanglement via noise the two LL-leads can be coupled further to Fermi liquid leads. In such a setup the LL-leads then would act as QDs [45]. Another way to prove spin-entanglement is to carry out spin-dependent current-current correlation measurements between the two LLs. Such spin dependent currents can be measured e.g. via spin filters (Sec. 4).

2.2. Triple-quantum dot entangler

In a third proposal [17], described in Fig. 2, the pair of spin-entangled electrons is provided by the singlet ground state of a single quantum dot D_C with an even number of electron [46]. In the Coulomb blockade regime [32], electron interactions in a dot create a large charging energy U that provides the energy filtering necessary for the suppression of the non-entangled currents. These arise either from the escape of the pair to the same lead, or from the transport of a single electron. The idea is to create a resonance for the joint

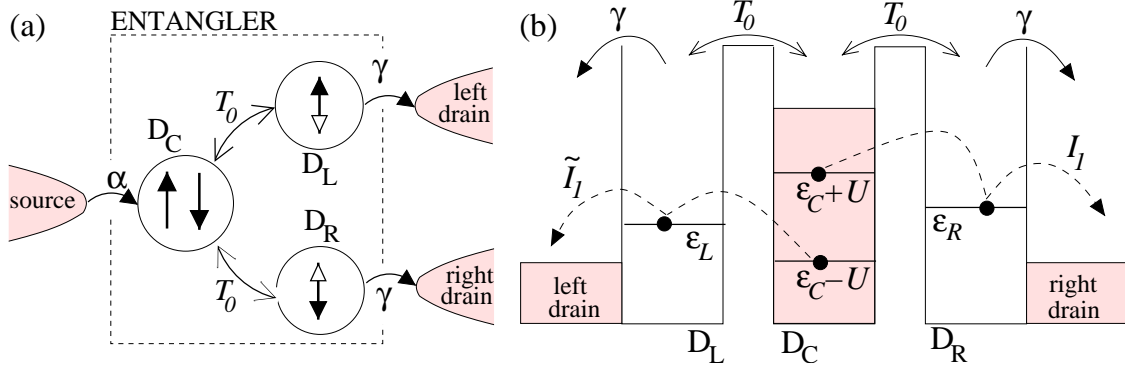


Figure 2. (a) Setup of the triple quantum dot entangler. The central dot D_C can accept 0, 1 or 2 electrons provided with rate α from the source lead l_C . Its ground state with 2 electrons is the spin singlet. The electrons can tunnel coherently (with tunnelling amplitudes T_0) between D_C and the two secondary dots D_L and D_R , which can only accept 0 or 1 electron and act as energy filters. Each electron from the singlet pair can finally tunnel out to the drain leads l_L and l_R with a rate γ . (b) Energy level diagram (single-particle). The dashed arrows represent the single-electron currents I_1 and \tilde{I}_1 . Adapted from [17, 23].

transport of the two electrons from D_C to secondary quantum dots D_L and D_R , similarly to the resonance described in Sec. 2.1.1. For this, we need the condition $\epsilon_L + \epsilon_R = 2\epsilon_C$, where ϵ_L and ϵ_R are the energy levels of the available state in D_L and D_R , and $2\epsilon_C$ is the total energy of the two electrons in D_C . On the other hand, the transport of a single electron from D_C to D_L or D_R is suppressed by the energy mismatch $\epsilon_C \pm U \neq \epsilon_L, \epsilon_R$, where $\epsilon_C \pm U$ is the energy of the 2nd/1st electron in D_C [47].

We describe the incoherent sequential tunneling between the leads and the dots in terms of a master equation [48] for the density matrix ρ of the triple-dot system (valid for $k_B T > \gamma$). The stationary solution of the master equation is found with MAPLE, and is used to define stationary currents. Besides the entangled current I_E coming from the *joint* transport of the electrons from D_C to D_L and D_R , the solitary escape of one electron of the singlet can create a non-entangled current I_1 , as it could enable a new electron coming from the source lead to form a new spin-singlet with the remaining electron. Another non-entangled current \tilde{I}_1 can be present if only one electron is transported across the triple-dot system; see Fig. 2(b). The definition of entangler *qualities* $Q = I_E/I_1$ and $\tilde{Q} = I_E/\tilde{I}_1$ enables us to check the suppression of these non-entangled currents.

In Fig. 3 we present results in the case where $\epsilon_R = \epsilon_C$. In (b) we see the two-electron resonance at $\epsilon_L = \epsilon_C = \epsilon_R$, which creates mobile entangled electrons with the same orbital energy (as required in the beam-splitter setup to allow entanglement detection; see Section 3). The exact analytical expressions are extremely lengthy, but we can get precise conditions for an efficient entangler regime by performing a Taylor expansion in terms of α, γ, T_0 (defined in Fig. 2). Introducing the conditions $Q, \tilde{Q} > Q_I^{\min}$ away from resonance ($\epsilon_L \neq \epsilon_C$) and $Q, \tilde{Q} > Q_{II}^{\min}$ at resonance ($\epsilon_L = \epsilon_C$), we obtain the conditions [17]

$$|\epsilon_L - \epsilon_C| < 2T_0/\sqrt{Q_I^{\min}}, \quad (6)$$

$$\gamma\sqrt{Q_{II}^{\min}/8} < T_0 < U\sqrt{4\alpha/\gamma Q_{II}^{\min}}, \quad (7)$$

illustrated in Fig. 3(b) and (c). We need a large U for the energy suppression of the one-electron transport, and $\gamma \ll T_0$ because the joint transport is a higher-order process in T_0 . The current saturates to $I_E \rightarrow e\alpha$ when $T_0^4 \gg U^2\gamma\alpha/32$ [see Fig. 3(d)]: then, the bottleneck process is the tunneling of the electrons from the source lead to the central dot. We see in (a) that equal currents in the left and right drain lead, $I_L = I_R$, are characteristic of the resonance $\epsilon_L = \epsilon_C$, which provides an experimental procedure to locate the efficient regime.

Taking realistic parameters for quantum dots [32, 49] such as $I_E = 20$ pA, $\alpha = 0.1$ μ eV and $U = 1$ meV, we obtain a maximum entangler quality $Q_{II}^{\min} = 100$ at resonance, and a finite width $|\epsilon_L - \epsilon_C| \simeq 6$

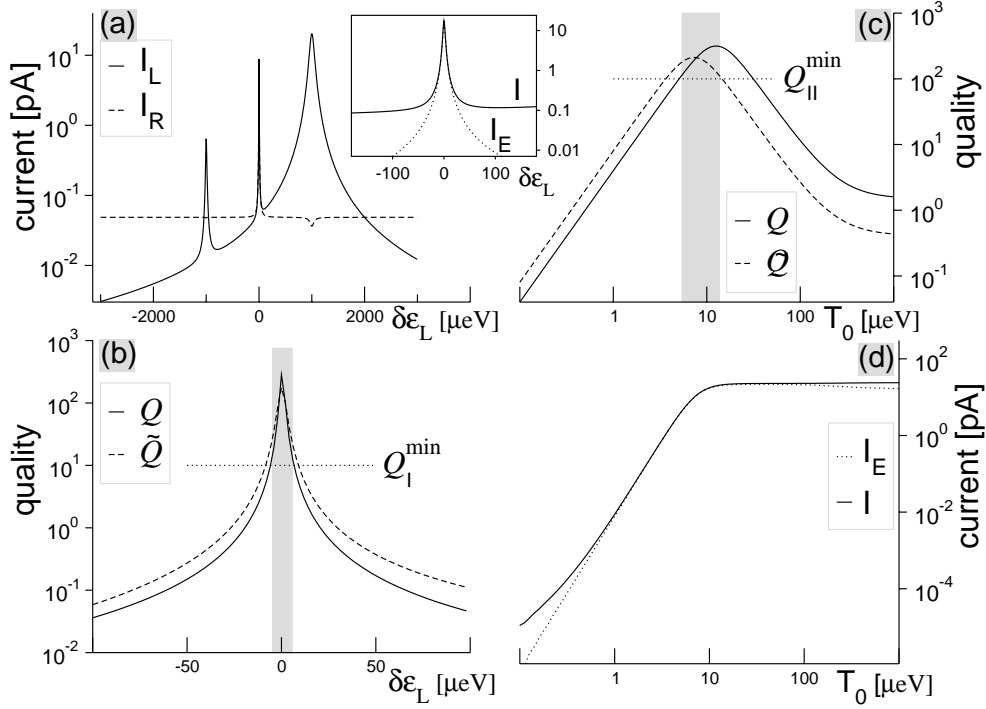


Figure 3. Quality and current of the triple-dot entangler, We take the parameters $\alpha = 0.1, \gamma = 1, T_0 = 10, U = 1000$ in μeV . (a) Entangled and non-entangled current in the left (I_L) and in the right (I_R) drain leads. The inset shows the resonance in a larger scale. (b) Quality Q and \tilde{Q} , around the resonance at $\epsilon_L - \epsilon_C = 0$ where the entangled current dominates. In gray, the width of the resonance defined by $Q, \tilde{Q} > Q_I^{\text{min}} = 10$ is $|\epsilon_L - \epsilon_C| < 6 \mu\text{eV}$, as predicted by Eq.(6). (c) Q and \tilde{Q} as a function of T_0 at resonance ($\epsilon_L = \epsilon_C$). In gray, the region where the quality of the entangler is $Q, \tilde{Q} > Q_{II}^{\text{min}} = 100$ corresponding to Eq. (7). (d) Saturation of the entangled current I_E . Adapted from [17].

μeV where the quality is at least $Q_I^{\text{min}} = 10$. It is crucial to avoid resonances with excited levels E' in D_L or D_R , as this could allow the undesired unentangled one-electron transport. In order to maintain a 90% efficiency, one needs a minimum distance of $\sim U/5$ between E' and the level of the second electron in D_C . This can be achieved by tuning the excited levels away with the help of a perpendicular magnetic field. To avoid completely the excited levels requires large energy levels spacings $\Delta\epsilon \simeq 2U$, which can be found in vertical quantum dots or carbon nanotubes [32]. Finally, we can estimate the relevant timescales by simple arguments. The entangled pairs are delivered every $\tau_{\text{pairs}} \simeq 2/\alpha \simeq 15$ ns. The average separation between two entangled electrons within one pair is given by the time-energy uncertainty relation: $\tau_{\text{delay}} \simeq 1/U \simeq 0.6$ ps, while their maximum separation is given by the variance of the exponential decay law of their escape into the leads: $\tau_{\text{max}} \simeq 1/\gamma \simeq 0.6$ ns. In conclusion, the singlet spin state is preserved throughout the transport process as τ_{delay} and τ_{max} are both well below reported spin decoherence times (in bulk) of 100 ns [11].

3. Detecting electronic entanglement

So far, photonic entanglement has been successfully demonstrated in various experiments, and used to exhibit quantum non-locality via Bell's inequality measurements [50] as well as quantum communication schemes such as teleportation or cryptography [51]. Here we address similar issues regarding the demonstration of electron spin entanglement in a mesoscopic system. The main idea is to exploit the unique relation between the symmetry of the orbital state and the spin states, which allows a detection of the spin state via measurements of the charge (orbital) degree of freedom of the electrons. More precisely, information

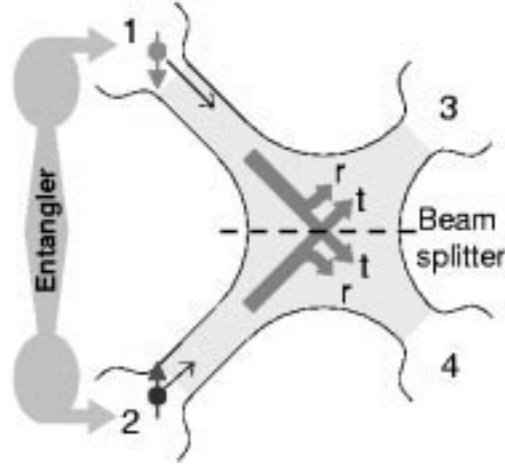


Figure 4. Beam-splitter for the detection of entangled electrons. An entangler (see Section 2) feeds a pair of entangled electrons, one in lead 1 and the other one in lead 2. The beam-splitter mixes the two current in order to induce scattering interferences; t, r are the transmission and reflection amplitudes. The resulting noise is measured in leads 3 and 4. One finds an enhanced noise (bunching) if the entangler provides spin-singlets $|S\rangle$ or, on the contrary, noise reduction if the entangler provides the entangled spin triplets $|T_0\rangle$. One also obtains noise reduction if non-entangled triplets $|T_{\pm}\rangle$ are simultaneously injected. The reference noise is the shot noise found in a single channel. Adapted from [18, 19].

beyond the average current is required, and one must consider the particle-particle correlations found in noise measurements [52, 53].

It has been known for a long time [54, 55] that increased correlations in the particle current (i.e., noise) are found for bosons (such as photons) going through a beam-splitter; such phenomenon has been termed “bunching”. Recently, the opposite behaviour for fermions (called “antibunching”) has been demonstrated experimentally for electrons in mesoscopic systems [56], as well as for free electrons [57]. However, it is in fact the symmetry of only the orbital part of the two-particle wavefunction which is relevant for the noise; hence one should expect antibunching only for two particles whose spins are in one of the three triplet states $|T_0\rangle = (|\uparrow\downarrow\rangle + |\downarrow\uparrow\rangle)/\sqrt{2}$, $|T_{\pm}\rangle = |\uparrow\uparrow\rangle, |\downarrow\downarrow\rangle$. On the other hand, a spin singlet state $|S\rangle = (|\uparrow\downarrow\rangle - |\downarrow\uparrow\rangle)/\sqrt{2}$ has a symmetric orbital wave function, which should therefore exhibit bunching. Hence, observing an increase of the noise of particles indicate bunching and, consequently, an entangled spin-singlet, while a decrease corresponds to antibunching and a spin-triplet state, which can be entangled or unentangled [18].

3.1. Noise in a beam-splitter setup

We assume that an entangler (for instance, one of the three proposals of Section 2) generates pairs of entangled electrons which are directly injected in the two incoming arms (leads 1 and 2) of a beam-splitter; see Fig. 4. The goal of the beam-splitter is to create two-particle interference effects, by allowing electrons to be transmitted (lead 1 \rightarrow lead 4 or 2 \rightarrow 3) with an amplitude t , or to be reflected (1 \rightarrow 3 or 2 \rightarrow 4) with an amplitude r . Here we neglect back-scattering (1 \rightarrow 1, 1 \rightarrow 2, 2 \rightarrow 1 or 2 \rightarrow 2), which is considered in Ref. [20]. Then conservation of probability reads $T + R = 1$ with $T = |t|^2$, $R = |r|^2$. The quantity of interest in this setup is the noise (the current-current correlation) measured in lead 3 (autocorrelation), or between leads 3 and 4 (cross-correlation).

We calculate transport quantities using the standard scattering theory [53] for non-interacting particles [58], at zero temperature and for zero bias. We consider the entangled incident states in leads 1 and 2

$$|\psi_{T/S}\rangle = \frac{1}{\sqrt{2}} \left(a_{\mathbf{q},1,\uparrow}^\dagger a_{\mathbf{q}',2,\downarrow}^\dagger \pm a_{\mathbf{q},1,\downarrow}^\dagger a_{\mathbf{q}',2,\uparrow}^\dagger \right) |\Psi_0\rangle \quad (8)$$

corresponding to a spin triplet (+) or singlet (-). Here $|\Psi_0\rangle$ denotes the filled Fermi sea in both leads, and

$a_{\mathbf{q},l,\sigma}^\dagger$ is the creation operator for an electron in lead l with momentum \mathbf{q} and spin σ . We consider that only one transverse channel is available in each lead, so that \mathbf{q}, \mathbf{q}' translates into the two energies ϵ, ϵ' of the incoming electrons. The unpolarized current operator for lead l can be written as [53]

$$\hat{I}_l(t) = \frac{e}{h\nu} \sum_{\sigma\epsilon\epsilon'} \left(a_{\epsilon,l,\sigma}^\dagger a_{\epsilon',l,\sigma} - b_{\epsilon,l,\sigma}^\dagger b_{\epsilon',l,\sigma} \right) e^{i(\epsilon-\epsilon')t/\hbar}, \quad (9)$$

with ν the density of states in the leads. The operator $a_{\epsilon,l,\sigma}^\dagger$ creates an incoming electron with energy ϵ , while $b_{\epsilon,l,\sigma} = \sum_{l'} \mathcal{S}_{l'l} a_{\epsilon,l',\sigma}$ correspond to outgoing electrons. The scattering matrix $\mathcal{S}_{l'l'}$ is assumed to be spin- and energy-independent, and reads $t = \mathcal{S}_{41} = \mathcal{S}_{32}, r = \mathcal{S}_{42} = \mathcal{S}_{31}, \mathcal{S}_{12} = \mathcal{S}_{34} = \mathcal{S}_{ll} = 0$. Note that the average current $|\langle \hat{I}_l \rangle| = e/h\nu$ does not depend on the orbital symmetry of the wavefunction. Introducing the fluctuations $\delta \hat{I}_l = \hat{I}_l - \langle \hat{I}_l \rangle$, we define their spectral density $S_{l'l'}(\omega)$ between leads l and l' and calculate it for an incoming state $|\psi_{T/S}\rangle$:

$$S_{l'l'}(\omega) = \lim_{\tau \rightarrow \infty} \frac{h\nu}{\tau} \int_0^\tau dt e^{i\omega t} \text{Re} \langle \psi_{T/S} | \delta \hat{I}_l \delta \hat{I}_{l'} | \psi_{T/S} \rangle. \quad (10)$$

For the noise at zero frequency ($\omega = 0$) we obtain [18]

$$S_{33} = S_{44} = -S_{34} = 2 \frac{e^2}{h\nu} T(1-T)(1 \mp \delta_{\epsilon\epsilon'}). \quad (11)$$

Here the upper sign corresponds to an incoming pair in one of the spin triplets states (entangled or not), while the lower sign corresponds to a spin singlet. This result contains the standard shot noise [53] $S = 2e^2 T(1-T)$ found for uncorrelated particles going through a tunnel barrier in one channel. The second term depends crucially on the spin state, and yields a doubling of the shot noise for singlets (bunching), and a suppression to zero noise for triplets (antibunching). Note that the δ_{ij} function requires to have electrons injected with the same energies $\epsilon = \epsilon'$; this is due to the Pauli exclusion principle which only applies for identical quantum states. Note that $S_{33} = -S_{34}$ is simply due to conservation of particles numbers and the absence of backscattering.

The result described above has recently been generalized for arbitrary incoming two-electron (mixed) spin states χ entering the beam-splitter [20]. A lower bound for the entanglement of formation E of pairs of electron spins injected into a mesoscopic conductor can be determined in terms of S_{33} from the inequality

$$E(\chi) \geq E(F) = H_2(1/2 + \sqrt{F(1-F)}), \quad (12)$$

where $H_2(x) = -x \log x - (1-x) \log(1-x)$ is the dyadic Shannon entropy and $F = S_{33}/4eIT(1-T)$. The lower bound can also be expressed in terms of the cross-correlators, which turn out to be more robust against backscattering from the beamsplitter [20]. A variable inhomogeneous magnetic field gives rise to a useful lower bound for the entanglement of arbitrary states. Spin relaxation (T_1 processes) and decoherence (T_2) during the ballistic coherent transmission of carriers can also be taken into account within Bloch theory, leading to a reduction of the entanglement of formation during the transmission through the beamsplitter.

In conclusion, performing noise measurements in the outgoing leads of the beam-splitter presented in Fig. 4 can uniquely indicate a spin-singlet state; moreover, a lower bound for a measure of entanglement (the entanglement of formation) can be directly inferred from the noise power. Distinguishing between the entangled and unentangled triplet states requires either a single-spin measurement (which could be accomplished using a single-spin measurement device discussed in Sec. 4) or a single-spin rotation in the ingoing arm. In both cases, the presence of spin-orbit interaction can help [19], which will be explained in more details in the next Section.

3.2. Beam-splitter with local Rashba interaction

An extension of the beam-splitter proposal discussed above is to consider a spin-orbit Rashba interaction [59, 3] as a means to rotate one of the spins. This offers the possibility to continuously change from bunching to antibunching, and find therefore a modulation in the noise signal, which is easier to observe

than a doubling or reduction as above. We consider a local Rashba interaction in one of the incoming leads (say, lead 1) over a finite length L . Such interaction is present in low-dimensional systems with structural inversion asymmetry, and arises from the gradient of the confining potential at the interface between two different materials. Importantly, its strength (denoted by the spin-orbit constant α) can be controlled via the voltage of external top and back gates defining the asymmetry [60]. The effect of the spin-orbit interaction is to coherently rotate the spin. For instance, an electron entering the Rashba region in a spin-up state will emerge with also a spin-down component [19]:

$$|\uparrow\rangle \longrightarrow \cos \theta_R/2 |\uparrow\rangle + \sin \theta_R/2 |\downarrow\rangle \quad (13)$$

up to an irrelevant global phase factor. Here we have introduced the Rashba angle $\theta_R = 2m\alpha L/\hbar^2$. It is then clear that rotating only one spin will change the state from a spin-singlet to a superposition of the different triplets. This is reflected in the expression for the noise [19]:

$$S_{33}(\theta_R) = 2 \frac{e^2}{h\nu} T(1-T) \times \begin{cases} 1 + \delta_{\epsilon\epsilon'} \cos \theta_R & , \text{ singlet } |S\rangle \\ 1 - \delta_{\epsilon\epsilon'} \cos \theta_R & , \text{ triplet } |T_0\rangle \\ 1 - \delta_{\epsilon\epsilon'} \cos^2(\theta_R/2) & , \text{ triplet } |T_{\pm}\rangle \end{cases} . \quad (14)$$

Here all the spin-states are defined along the z axis perpendicular to the plane of transport. As a consequence, a noise measurement will display a sinusoidal modulation as a function of θ_R , which can be varied via α , provided that one injects a pair of entangled electrons (in state $|S\rangle$ or $|T_0\rangle$) with the same orbital energy $\epsilon = \epsilon'$.

4. A quantum dot as a spin filter, a spin memory, and a probe of single-spin decoherence

Crucial building blocks needed for quantum computation and communication comprise single-spin measurement devices, spin-filters and read-out devices for a spin-memory. As we shall see below, such devices can be implemented with a quantum dot in the Coulomb blockade regime. The essential component is a spin-filter, which only lets through electrons with specific spin direction (say, \uparrow). With such an apparatus one could think of a single-spin measurement device, obtained by coupling the spin-filter to a single-electron transistor [61], so that one has a large current through the transistor only if the single spin was in the specified direction, and was therefore allowed to pass through the spin-filter.

We use similar approaches for the discussion of the different devices below, based on a tunneling Hamiltonian, and first- and second-order approximations. At resonance, the dominant contribution I_s to the current arises from sequential tunneling (ST) [32]; it corresponds to first-order tunneling between the leads and the dot, and the electron number on the dot fluctuates. The smaller second-order contribution is the cotunneling (CT) current I_c [62], where the number of electrons on the dot only changes in the virtual intermediate state. An important requirement is that the spin-degeneracy must be lifted with *different* Zeeman splittings in the dot and in the leads, e.g. by applying local magnetic fields or by using materials with different effective g factors for leads and dot. Also, we consider small dots with large energy-level spacings $\delta > \Delta\mu = \mu_1 - \mu_2 > 0, k_B T$, where $\mu_{1,2}$ are the chemical potentials of the source and drain lead.

4.1. Spin filter

The spin-filter [21] is described in Fig. 5(a). It is important to have a Zeeman splitting which is negligible in the leads and only significant in the dot, where it is $\Delta_z = \mu_B |gB|$. We consider an odd number of electrons in the dot, with a total spin 1/2 (shell filling of singlet states). Because of the Zeeman coupling, the topmost electron is in the spin ground state $|\uparrow\rangle$. In the sequential tunneling regime ($\mu_1 > E_S > \mu_2$) the only state accessible for transport is the spin singlet with energy E_S . Thus, only electrons with spin \downarrow can tunnel onto and off the dot, implying that the outgoing current I_s is spin- \downarrow polarized.

However, one should also check the small cotunneling contribution to the current, I_c , which can contain a spin- \uparrow component. This potentially reduces the efficiency of the spin-filtering effect. We find a degree of

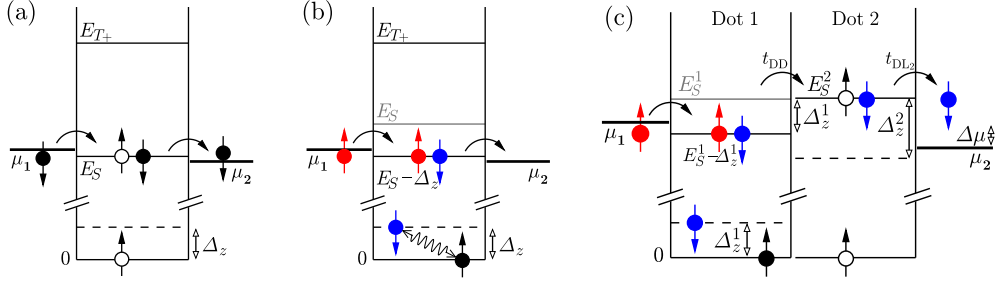


Figure 5. (a) A spin filter from a quantum dot. The dot is in the sequential tunneling regime, $\mu_1 > E_S > \mu_2 > E_S - \Delta_z$, and coupled to unpolarized leads with chemical potentials $\mu_{1,2}$. The singlet/triplet levels are E_S/E_{T+} (counting from $E_{\uparrow} = 0$) and the Zeeman splitting (only in the dot) is $\Delta_z = g\mu_B B_z$. (b) Setup to measure single-spin decoherence time, obtained by shifting the energy levels such that $E_S > \mu_1 > E_S - \Delta_z > \mu_2$. If initially the spin-state on the dot is $|\uparrow\rangle$, sequential tunneling is blocked by energy conservation. An ESR pulse (Rabi flip, drawn as wavy line) can excite the dot and unblock it for spin \uparrow electrons coming from lead 1. Finally, spin \uparrow or \downarrow electrons can tunnel from the singlet state into lead 2. (c) Spin inverter (combined setup). The spin state of dot 1 switches the current as in (b), while the second dot 2 acts as a spin filter, in the regime $E_S^1 \approx E_S^2$, $E_S^1 > \mu_1 > E_S^1 - \Delta_z^1$, $E_S^2 > \mu_2 > E_S^2 - \Delta_z^2$, $|t_{DD}| < |t_{DL_2}|$, $\Delta_z^1 \approx \Delta_z^2$. This allows the transition sequence $\uparrow (\uparrow)_1 (\uparrow)_2 \xrightarrow{\text{ESR}} \uparrow (\downarrow)_1 (\uparrow)_2 \rightarrow (\downarrow)_1 (\uparrow)_2 \rightarrow (\uparrow)_1 (\downarrow)_2 \rightarrow (\uparrow)_1 (\uparrow)_2 \downarrow$. Adapted from [24, 21, 22].

spin-polarization [21]

$$\frac{I_s(\downarrow)}{I_c(\uparrow)} \sim \frac{\min\{\Delta_z^2, (E_{T+} - E_S)^2\}}{\gamma \max\{kT, \Delta\mu\}}, \quad (15)$$

where we considered equal tunneling rates γ between the dot and both source and drain leads. The ST regime corresponds to $\gamma < kT, \Delta\mu$; if in addition $kT, \Delta\mu < \Delta_z, |E_{T+} - E_S|$, the ratio Eq. (15) is large and the spin-filter is efficient. Such a spin filter has a broad range of applications, as it could provide highly spin-polarized current as required by most spintronics devices [1].

4.2. Read-out of a spin memory

Here we consider the storage a bit of information in a single-spin in a quantum dot (a “spin-memory”), for which one needs ways to read out the spin-state. This could be performed with a setup similar to the spin-filter: one merely needs to connect it to spin-polarized leads [5], which will be able to pass electrons through the dot only if the polarization is opposite from the single-spin state [21].

We consider the situation where the spin polarization in both leads is \uparrow . If the dot (the spin-memory) is in state $|\downarrow\rangle$, the electrons of the source lead are allowed to tunnel onto the dot by forming a singlet, and then to tunnel out to the other lead, creating a finite current $I_s \neq 0$. Since the leads can only absorb spin-up electrons, these are the only allowed sequential tunneling transitions, i.e. $\uparrow \downarrow \rightarrow \uparrow \downarrow \rightarrow \downarrow \uparrow$. However, if the dot is in state $|\uparrow\rangle$, no electron can tunnel onto the dot because the formation of the triplet is forbidden by energy conservation, and one has no ST current, $I_s = 0$ —although there is a small cotunneling leakage current $I_c \neq 0$. The ratio I_s/I_c is given by Eq. (15), where the numerator becomes $(E_{T+} - E_S + \Delta_z)^2$ (since here only the CT-process with an intermediate triplet state is possible). Therefore, the initial spin state of the quantum dot can be detected by measuring the charge current through the dot.

The measurement efficiency can also be quantified by a detailed analysis of the read-out procedure [22]. For a dot with spin $|\downarrow\rangle$, the probability for no electron being transmitted after a time t decreases exponentially: $P_1(t) = \exp(-\gamma t)(1 + \gamma t)$. For example, after a time $t = 2e/I$ the spin state can be determined with more than 90% probability [22]. For a typical sequential tunneling current on the order of 0.1 – 1 nA [32], this measuring time is 0.3 – 3 ns.

4.3. Detection of single-spin decoherence

We have proposed a setup where, by applying an ESR field to the dot-spin, the single spin decoherence time T_2 can be determined by the line shape of the (stationary) sequential tunneling current through the dot [22]. In this setup, the Zeeman splitting on the dot is large, $\Delta_z = g\mu_B B > \Delta\mu, kT$, and different from the Zeeman splitting of the leads, $\Delta_z^{\text{leads}} \not\approx \Delta_z$. The energy levels are tuned such that no sequential tunneling current flows through the dot when it is in its ground state $|\uparrow\rangle$, see Fig. 5(b). However, if an ESR field is present and produces Rabi-flips on the dot, current will flow through the dot involving state $|\downarrow\rangle$. By calculating the stationary solution of the master equation within the rotating wave approximation we find for the stationary current [22]

$$I(\omega) \propto \frac{V_{\downarrow\uparrow}}{(\omega - \Delta_z)^2 + V_{\downarrow\uparrow}^2}. \quad (16)$$

Thus, the current as a function of the ESR frequency ω has a resonant peak at $\omega = \Delta_z$ and width $2V_{\downarrow\uparrow} = \gamma_{S\uparrow} + \gamma_{S\downarrow} + 2/T_2$. Here, $\gamma_{S\sigma}$ denotes the rate for an electron to tunnel from a lead into the dot which was initially in state $|\sigma\rangle = |\uparrow\rangle, |\downarrow\rangle$. Thus, the linewidth of the current provides a lower bound on the intrinsic single-spin decoherence time T_2 . For weak tunneling $\gamma_{S\sigma} < 2/T_2$, this bond saturates, i.e. the width of the peak becomes $2/T_2$. For finite temperatures in the linear response regime $\Delta\mu < kT$, the current has roughly the standard sequential tunneling peak shape $\cosh^{-2}[(E_S - E_\downarrow - \mu)/2kT]$ with $\mu = (\mu_1 + \mu_2)/2$, while the resonant structure of $I(\omega)$ [Eq. (16)] remains unaffected. At last we point out that if this setup is operated at zero bias $\Delta\mu = 0$, only electrons with spin \uparrow can tunnel onto the dot and only with spin \downarrow off the dot. Thus, the leads become locally spin-polarized. This concentration gradient acts as effective spin-dependent chemical potential, leading to a finite spin-current while there is no charge current. Such spin-currents can be detected e.g. via the (finite) noise of the charge current [18].

Furthermore, this device allows a time-resolved measurement of the spin state of the dot. This allows to detect the Rabi oscillations of a single spin and the Zeno effect via the current $I_s(t)$ [22]. In order to measure $I_s(t)$ an ensemble average is required, e.g. by using an array of (independent) dots or by time-series measurement over a single dot.

4.4. Pumping

The setup described in the previous section can be used as an electron *pump* if one allows for spin-dependent tunneling rates $\gamma_l^\uparrow \neq \gamma_l^\downarrow$ between dot and lead l for electrons with spin \uparrow, \downarrow [22]. The current at zero bias $\Delta\mu = 0$ is driven with an externally applied ESR source and is proportional to $\gamma_1^\uparrow \gamma_2^\downarrow - \gamma_1^\downarrow \gamma_2^\uparrow$.

Spin-dependent tunneling rates are produced by spin-polarized leads [21], by spin-dependent tunneling barriers or by the combined setup shown in Fig. 5(c). This setup uses an additional quantum dot as spin filter and acts as a “spin inverter” which takes spin up electrons as input and produces spin down electrons as output.

5. Conclusion

We have proposed and theoretically analyzed devices which address a number of milestones of quantum communication protocols with electron spins in mesoscopic systems. For the creation of EPR-pairs, we have proposed three different schemes for the preparation of spin-singlet electron pairs, and their injection into solid-state quantum channels. In the second part, we have discussed an interference device able to distinguish, via noise measurement, the entangled spin singlet from the spin triplet states. A local spin-orbit interaction extends this proposal by allowing a continuously variable noise signature, controllable by external gates. Finally, we have shown how one can use single quantum dots as fundamental tools for accessing quantum information stored as a single spin. We have described a spin-filter, a spin-memory read-out, and, finally, a device able to estimate the decoherence rate of a single-spin in a quantum dot —a crucial parameter for the coherent manipulation of the fundamental quantum system that is an electron spin.

Acknowledgments

We would like to thank E.V. Sukhorukov for his contribution to the work presented here. Financial support from NCCR “Nanoscale Science”, Swiss NSF, U.S. DARPA and ARO is gratefully acknowledged.

References

- [1] G.A. Prinz, *Phys. Today*, **48**, (1995), 58; *Science*, **282**, (1998), 1660; D.D. Awschalom, M.E. Flatte, and N. Samarth, *Sci. Am.*, **286**, (2002), 66.
- [2] *Semiconductor Spintronics and Quantum Computation*, Eds. D.D. Awschalom, D. Loss, and N. Samarth (Springer, Berlin, 2002).
- [3] S. Datta and B. Das, *Appl. Phys. Lett.*, **56**, (1990), 665.
- [4] J. Schliemann, J.C. Egues, and D. Loss, *Phys. Rev. Lett.*, **90**, (2003), 146801.
- [5] R. Fiederling, M. Keim, G. Reuscher, W. Ossau, G. Schmidt, A. Waag, and L.W. Molenkamp, *Nature*, **402**, (1999), 787; Y. Ohno, D.K. Young, B. Beschoten, F. Matsukura, H. Ohno, and D.D. Awschalom, *Nature*, **402**, (1999), 790.
- [6] I. Malajovich, J.M. Kikkawa, D.D. Awschalom, J.J. Berry, and N. Samarth, *Phys. Rev. Lett.*, **84**, (2000), 1015; I. Malajovich, J.J. Berry, N. Samarth, and D.D. Awschalom, *Nature*, **411**, (2001), 770.
- [7] M. Johnson and R. H. Silsbee, *Phys. Rev. Lett.*, **55**, (1985), 1790; *Phys. Rev. B*, **37**, (1988), 5326; F.J. Jedema, H.B. Heersche, A.T. Filip, J.J.A. Baselmans, and B.J. van Wees, *Nature*, **416**, (2002), 713.
- [8] A. Steane, *Rep. Prog. Phys.*, **61**, (1998), 117.
- [9] D. Loss and D.P. DiVincenzo, *Phys. Rev. A*, **57**, (1998), 120.
- [10] C.H. Bennett and D.P. DiVincenzo, *Nature*, **404**, (2000), 247.
- [11] J.M. Kikkawa, I.P. Smorchkova, N. Samarth, D.D. Awschalom, *Science*, **277**, (1997), 1284; J.M. Kikkawa and D.D. Aschwalom, *Phys. Rev. Lett.*, **80**, (1998), 4313; J.M. Kikkawa and D.D. Aschwalom, *Phys. Today*, **52**, (1999), 33.
- [12] A. Einstein, B. Podolsky, and N. Rosen, *Phys. Rev.*, **47**, (1935), 777.
- [13] J.S. Bell, *Rev. Mod. Phys.*, **38**, (1966), 447.
- [14] J. Schliemann, J.I. Cirac, M. Kus, M. Lewenstein, D. Loss, *Phys. Rev. A*, **64**, (2001), 022303.
- [15] P. Recher, E.V. Sukhorukov, and D. Loss, *Phys. Rev. B*, **63**, (2001), 165314.
- [16] P. Recher and D. Loss, *Phys. Rev. B*, **65**, (2002), 165327.
- [17] D. S. Saraga and D. Loss, *Phys. Rev. Lett.*, **90**, (2003), 166803.
- [18] G. Burkard, D. Loss, and E.V. Sukhorukov, *Phys. Rev. B*, **61**, (2000), R16303.
- [19] J.C. Egues, G. Burkard, and D. Loss, *Phys. Rev. Lett.*, **89**, (2002), 176401; J.C. Egues, G. Burkard, and D. Loss, *J. Superconductivity*, **16**, (2003), 711.
- [20] G. Burkard and D. Loss, *Phys. Rev. Lett.*, **91**, (2003), 087903.
- [21] P. Recher, E.V. Sukhorukov, and D. Loss, *Phys. Rev. Lett.*, **85**, (2000), 1962.
- [22] H.-A. Engel and D. Loss, *Phys. Rev. Lett.*, **86**, (2001), 4648; *Phys. Rev. B*, **65**, (2002), 195321.
- [23] J.C. Egues, P. Recher, D.S. Saraga, V.N. Golovach, G. Burkard, E.V. Sukhorukov, and D. Loss, in Ref. [52].
- [24] H.-A. Engel, P. Recher, and D. Loss, *Solid State Commun.*, **119**, (2001), 229.

- [25] M.-S. Choi, C. Bruder, and D. Loss, *Phys. Rev. B*, **62**, 13569 (2000); cond-mat/0001011.
- [26] C. Bena, S. Vishveshwara, L. Balents, and M.P.A. Fisher, *Phys. Rev. Lett.*, **89**, (2002), 037901.
- [27] G.B. Lesovik, T. Martin, and G. Blatter, *Eur. Phys. J. B*, **24**, (2001), 287.
- [28] V. Bouchiat, N. Chtchelkatchev, D. Feinberg, G.B. Lesovik, T. Martin, J. Torres, *Nanotechnology*, **14**, (2003), 77.
- [29] R. Mélin, cond-mat/0105073.
- [30] W.D. Oliver, F. Yamaguchi, Y. Yamamoto, *Phys. Rev. Lett.* **88**, (2002), 037901.
- [31] S. Bose and D. Home, *Phys. Rev. Lett.*, **88**, (2002), 050401.
- [32] L.P. Kouwenhoven *et al.*, in *Mesoscopic Electron Transport*, NATO ASI Series E, Vol. 345 (Kluwer, Dordrecht, 1997).
- [33] J.M. Elzerman, R. Hanson, J.S. Greidanus, L.H. Willems van Beveren, S. De Franceschi, L.M.K. Vandersypen, S. Tarucha, and L.P. Kouwenhoven, *Phys. Rev. B*, **67**, (2003), 161308(R).
- [34] C.W.J. Beenakker, C. Emary, M. Kindermann, J.L. van Velsen, *Phys. Rev. Lett.*, **91**, (2003), 147901.
- [35] In principle, an entangler producing entangled triplets $|\uparrow\downarrow\rangle + |\downarrow\uparrow\rangle$ or *orbital* entanglement would also be desirable.
- [36] This condition reflects energy conservation in the Andreev tunnelling event from the SC to the two QDs.
- [37] This reduction factor of the current I_2 compared to the resonant current I_1 reflects the energy cost in the virtual states when two electrons tunnel via the same QD into the same Fermi lead and are given by U and/or Δ . Since the lifetime broadenings γ_1 and γ_2 of the two QDs 1 and 2 are small compared to U and Δ such processes are suppressed.
- [38] A.F. Volkov, P.H.C. Magnée, B.J. van Wees, and T.M. Klapwijk, *Physica C*, **242**, (1995), 261.
- [39] M. Kociak, A.Yu. Kasumov, S. Guéron, B. Reulet, I.I. Khodos, Yu.B. Gorbatov, V.T. Volkov, L. Vaccarini, and H. Bouchiat, *Phys. Rev. Lett.*, **86**, (2001), 2416.
- [40] M. Bockrath, D.H. Cobden, J. Lu, A.G. Rinzler, R.E. Smalley, T. Balent, and P.L. McEuen, *Nature*, **397**, (1999), 598; R. Egger and A. Gogolin, *Phys. Rev. Lett.*, **79**, (1997), 5082; R. Egger, *Phys. Rev. Lett.*, **83**, (1999), 5547; C. Kane, L. Balents, and M.P.A. Fisher, *Phys. Rev. Lett.*, **79**, (1997), 5086.
- [41] For a review see e.g. H.J. Schulz, G. Cuniberti, and P. Pieri, in *Field Theories for Low-Dimensional Condensed Matter Systems*, edited by G. Morandi *et al.* (Springer, 2000); or J. von Delft and H. Schoeller, *Annalen der Physik*, Vol. 4, (1998), 225.
- [42] The interaction dependent constants A_b are of order one for not too strong interaction between electrons in the LL but are decreasing when interaction in the LL-leads is increased [16]. Therefore in the case of substantially strong interaction as it is present in metallic carbon nanotubes, the pre-factors A_b can help in addition to suppress I_2 .
- [43] Since $\gamma_{\rho-} > \gamma_{\rho+}$, it is more probable that two electrons coming from the same Cooper pair travel in the same direction than into different directions when injected into the same LL-lead.
- [44] L. Balents and R. Egger, *Phys. Rev. B*, **64**, (2001), 035310.
- [45] In order to have exclusively singlet states as an input for the beamsplitter setup, it is important that the LL-leads return to their spin ground-state after the injected electrons have tunnelled out again into the Fermi leads. For an infinite LL, spin excitations are gapless and therefore an arbitrary small bias voltage μ between the SC and the Fermi liquids gives rise to spin excitations in the LL. However, for a realistic finite size LL (e.g. a nanotube), spin excitations are gapped on an energy scale $\sim \hbar v_F/L$, where L is the length of the LL. Therefore, if $k_B T, \mu < \hbar v_F/L$ only singlets can leave the LL again to the Fermi leads, since the total spin of the system has to be conserved. For metallic carbon nanotubes, the Fermi velocity is $\sim 10^6$ m/s, which gives an excitation gap of the order of a few meV for $L \sim \mu\text{m}$; this is large enough for our regime of interest.

- [46] S. Tarucha, D. G. Austing, Y. Tokura, W.G. van der Wiel, and L.P. Kouwenhoven, *Phys. Rev. Lett.*, **84**, (2000), 2485. It might be necessary to apply a small magnetic field or to distort the confining potential to lift the orbital degeneracy which could favor the triplet state corresponding to Hund's rule. An alternative is to start with an empty dot, where the two-electron ground-state is a singlet; see e.g. N.W. Ashcroft and N.D. Mermin, *Solid State Physics* (Saunders College Publishing, 1976), Chap. 32.
- [47] This symmetric setup of the charging energy U (considered here for convenience of notation) is obtained when the gate voltages are tuned such that the total Coulomb charging energies in D_C are equal with zero or two electrons.
- [48] K. Blum, *Density Matrix Theory and Applications* (Plenum Press, New York, 1996).
- [49] T.H. Oosterkamp, T. Fujisawa, W.G. van der Wiel, K. Ishibashi, R.V. Hijman, S. Tarucha, L.P. Kouwenhoven, *Nature*, (London), **395**, (1998), 873; T. Fujisawa, T.H. Oosterkamp, W.G. van der Wiel, B.W. Broer, R. Aguado, S. Tarucha, L.P. Kouwenhoven, *Science*, **282**, (1998), 932.
- [50] A. Aspect, J. Delibard, and G. Roger, *Phys. Rev. Lett.*, **49**, (1982), 1804; W. Tittel, J. Brendel, H. Zbinden, and N. Gisin, *Phys. Rev. Lett.*, **81**, (1998), 3563.
- [51] D. Bouwmeester, J.W. Pan, K. Mattle, M. Eibl, H. Weinfurter, A. Zeilinger, *Nature*, **390**, (1997), 575; D. Boschi, S. Branca, F. De Martini, L. Hardy, and S. Popescu, *Phys. Rev. Lett.*, **80**, (1998), 1121.
- [52] For a review of recent advances regarding quantum noise, see Y.V. Nazarov (ed.), *Quantum Noise in Mesoscopic Physics*, NATO ASI Series II, Vol. 97 (Kluwer, 2003).
- [53] Ya. M. Blanter and M. Buttiker, *Phys. Rep.*, **336**, (2000), 1.
- [54] R. Hanbury Brown and R.Q. Twiss, *Nature*, **177**, (1956), 27.
- [55] R. Loudon, *Phys. Rev. A*, **58**, (1998), 4904.
- [56] R.C. Liu, B. Odom, Y. Yamamoto, and S. Tarucha, *Nature*, **391**, (1998), 263; W.D. Oliver, J. Kim, R.C. Liu, and Y. Yamamoto, *Science*, **284**, (1999) 299; M. Henny, S. Oberholzer, C. Strunk, T. Heinzel, K. Ensslin, M. Holland, and C. Schönberger, *Science* **284**, (1999), 296.
- [57] H. Kiesel, A. Renz, F. Hasselbach, *Nature*, **418**, (2002), 392.
- [58] The effect of the many-electron Coulomb interaction in the leads is only to renormalize the Green function (and thereby, the entangled state) by a factor $z_F = 0.66$ in a typical 2D GaAs material [18].
- [59] Yu.A. Bychkov and E.I. Rashba, *JETP Lett.*, **39**, (1984), 78.
- [60] G. Engels, J. Lange, T. Schäpers, and H. Lüth, *Phys. Rev. B*, **55**, (1997), R1958; J. Nitta, T. Akazaki, H. Takayanagi, and T. Enoki, *Phys. Rev. Lett.*, **78**, (1997), 1335; D. Grundler, *Phys. Rev. Lett.*, **84**, (2000), 6074; Y. Sato, T. Kita, S. Gozu, and S. Yamada, *J. Appl. Phys.*, **89**, (2001), 8017.
- [61] T.A. Fulton and G.J. Dolan, *Phys. Rev. Lett.*, **59**, (1987), 109.
- [62] D. V. Averin and Yu. V. Nazarov, in *Single Charge Tunneling*, eds. H. Grabert, M. H. Devoret, NATO ASI Series B, Vol. 294, Plenum Press, New York, 1992.